SERBIAN JOURNAL OF ELECTRICAL ENGINEERING
Vol. 23, No. 2, June 2026, 335-352

UDC: 537.531:621.395.721.5 **DOI: https://doi.org/10.2298/SJEE2602335T**

Original scientific paper

Analysis of Near-Field and Radiation Characteristics of a Mobile Phone in 4G and 5G Frequency Bands in the Presence of Shielding Structures

Ana Tatović[1]

Abstract: This paper presents a numerical investigation of the near-field and radiation characteristics of a mobile phone operating in 4G and 5G frequency bands. The analysis is performed at 1800 MHz, 2600 MHz, and 3500 MHz in the presence of shielding structures composed of materials with different electromagnetic properties. Three representative materials, namely aluminum, FR4, and a carbon-loaded polymer, are considered in order to evaluate the influence of conductive, dielectric, and lossy shielding configurations on the electromagnetic behavior of the device. The mobile phone model and shielding structures are developed and analyzed using the WIPL-D EM simulation software. The effects of shield material, shield distance, shield position, and phone orientation relative to the shielding plate are investigated through a comprehensive parametric study. The near-field behavior is evaluated using the electric field while the influence of the shielding structures on the antenna performance is examined through reflection coefficient, gain and radiation pattern analysis. The obtained results provide insight into the interaction between shielding structures and mobile phone antennas operating in contemporary wireless communication bands and may serve as guidelines for the design of shielding configurations that reduce near-field electromagnetic field levels while preserving acceptable antenna performance.

Keywords: Mobile phone antenna, Shielding structures, Near-field analysis, Electric field distribution, Reflection coefficient, Antenna gain, Radiation characteristics.

[1]University of Kragujevac, Faculty of Technical Sciences Čačak, Čačak, Serbia
ana.tatovic@ftn.kg.ac.rs, https://orcid.org/0000-0001-5653-0850

Colour versions of the one or more of the figures in this paper are available online at https://sjee.ftn.kg.ac.rs

1 Introduction

The rapid growth of wireless communications and the increasing demand for high data rates have accelerated the deployment of advanced fourth-generation (4G) and fifth-generation (5G) mobile communication systems. Modern mobile networks provide enhanced spectral efficiency, reduced latency, improved network capacity, and support for a wide range of emerging wireless services and applications [1, 2]. Among the currently deployed frequency bands, 1800 MHz and 2600 MHz are widely used for Long-Term Evolution (LTE) systems, while the 3500 MHz band has become one of the principal frequency bands for sub-6 GHz 5G communications [3]. The continuous expansion of mobile communication technologies has consequently increased interest in the electromagnetic fields generated by mobile devices operating in close proximity to users and surrounding electronic equipment.

Mobile phones represent one of the most widely used sources of radiofrequency electromagnetic fields in everyday environments. Since mobile devices are typically operated at short distances from the human body and nearby objects, the electromagnetic field distribution in the near-field region becomes particularly important. The characteristics of the generated fields depend on several factors, including the operating frequency, antenna geometry, device configuration, surrounding environment, and the presence of nearby conductive or dielectric structures [4, 5]. As communication systems continue to evolve toward higher frequencies and more complex antenna configurations, understanding the interaction between mobile phone antennas and nearby objects becomes increasingly significant for wireless device design and electromagnetic compatibility studies.

Numerous studies have investigated electromagnetic field propagation and radiation characteristics in contemporary wireless communication systems. Deaconescu et al. in [6] analyzed the temporal variations of electromagnetic fields radiated by mobile phones operating in 4G and 5G networks and highlighted the frequency-dependent behavior of emitted signals. In [7] authors reviewed the available research related to radiofrequency fields used in modern wireless communication systems and discussed the characteristics of electromagnetic exposure associated with emerging 5G technologies. In addition, electromagnetic fields generated by mobile phones have been investigated through numerical simulations and exposure analyses. A recent study published in [11] examined the distribution of the specific absorption rate (SAR) in a human head model during hands-free mobile phone usage at 900 MHz and 1800 MHz, demonstrating the importance of numerical modeling for evaluating electromagnetic interactions between mobile devices and their surrounding environment. Furthermore, several investigations have addressed the influence of shielding structures on electromagnetic field propagation and interference suppression. Metallic plates, conductive meshes, and composite materials have been widely employed in electromagnetic shielding applications due to their capability to modify field distributions and reduce electromagnetic interference [8, 15]. The effectiveness of such structures depends on the electromagnetic properties of the material, operating frequency, geometric configuration, and relative position with respect to the radiation source.

Despite extensive investigations into electromagnetic exposure assessment and shielding techniques, limited attention has been paid to the influence of shielding structures on the electromagnetic behavior of mobile phone antennas themselves. Most reported studies focus primarily on exposure metrics or shielding effectiveness, while the impact of shielding structures on antenna matching conditions, radiation efficiency, and field distribution is often considered separately. However, shielding structures placed in proximity to a mobile phone antenna may simultaneously alter the near-field distribution, modify antenna impedance characteristics, affect radiation efficiency, and change the overall radiation pattern. Consequently, the achieved reduction of electromagnetic field levels may be accompanied by degradation of antenna performance, making the interaction between shielding structures and mobile phone antennas a complex electromagnetic problem that requires further investigation. This issue becomes particularly important for contemporary 4G and 5G communication bands, where variations in operating frequency and wavelength may significantly influence the shielding mechanism and the resulting antenna behavior.

Recent studies have investigated various aspects of electromagnetic exposure and mobile phone performance in modern wireless communication systems. In [10], the influence of shielding structures and polarization effects on SAR levels at sub-6 GHz frequencies using layered human head models was investigated. The influence of mobile phone position on SAR distribution during hands-free operation was studied in [11]. Penta and Kumar in [12] proposed RF shielding structures based on ferrite and foam absorbers for reducing SAR in a 26 GHz PIFA antenna intended for 5G applications. More recently, [13] introduced a metasurface-loaded mobile phone cover capable of simultaneously reducing SAR and improving antenna radiation characteristics. [14] reviewed MIMO antennas for 5G smartphones, including SAR analysis and antenna performance, while [16] presented a comprehensive review of modern mobile phone antenna design. Although these studies significantly contribute to the understanding of electromagnetic exposure, shielding effectiveness, and antenna performance, most previous investigations considered these aspects separately. The main contribution of the present work lies in the integrated investigation of the near-field electric-field distribution and antenna characteristics in the presence of shielding structures. Furthermore, a comprehensive parametric analysis is performed by simultaneously considering the effects of shielding material properties, shield position, shield-to-antenna distance, mobile phone orientation, and operating frequency. Such an approach enables a more complete assessment of the interaction between shielding structures and mobile phone antenna performance in representative 4G and sub-6 GHz 5G frequency bands.

Motivated by these considerations, this paper investigates the interaction between shielding structures and a mobile phone antenna operating at 1800 MHz, 2600 MHz, and 3500 MHz, corresponding to representative 4G and 5G communication bands. Materials with substantially different electromagnetic properties, namely aluminum, FR4, and a carbon-loaded polymer, are considered in order to represent conductive, dielectric, and lossy shielding mechanisms. The analysis is performed using the WIPL-D electromagnetic simulation software and focuses on both the near-field behavior and the radiation characteristics of the mobile phone antenna. The influence of shielding material, shield position, shield distance, and device orientation are investigated in order to provide a better understanding of the electromagnetic mechanisms governing the interaction between shielding structures and mobile phone antennas. The obtained results may serve as useful guidelines for the design of shielding configurations intended to reduce near-field electromagnetic field levels while preserving acceptable antenna performance in modern wireless communication devices.

2 Mobile Phone Model and Shielding Configurations

The investigated model consists of a mobile phone equipped with a monopole antenna operating in representative 4G and 5G communication bands. Numerical simulations were performed using the WIPL-D software [9]. The objective of the study is to evaluate the influence of shielding structures with different electromagnetic properties on both the near-field distribution and the radiation characteristics of the mobile phone antenna.

The investigated mobile phone model and the shielding structure considered in this study are shown in Fig. 1. The dimensions of the mobile phone enclosure are 150 mm × 75 mm × 8 mm and it serves as the supporting structure for the antenna model. The shielding plate is positioned in proximity to the monopole antenna and is characterized by variable material properties, position, distance, and orientation relative to the mobile phone.

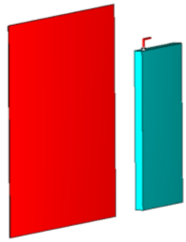

Fig. 1 – *Geometry of the mobile phone model with the shielding plate used in the parametric analysis.*

The observed frequencies correspond to widely deployed LTE and 5G communication bands and enable the investigation of shielding effects over a broad range of contemporary mobile communication services. To ensure resonant operation at each frequency band, the monopole dimensions were adjusted according to the corresponding center frequency. The resulting monopole dimensions are presented in **Table 1**.

Table 1
Monopole dimensions.

CENTER FREQUENCY [MHz]	MONOPOLE LENGTH [mm]
1800	42
2600	30.6
3500	23.5

Three shielding materials with significantly different electromagnetic properties were selected in order to investigate various shielding mechanisms. Aluminum was considered as a representative conductive material due to its high electrical conductivity and widespread use in electromagnetic shielding applications. FR4 was selected as a representative dielectric material commonly employed as a substrate and structural material in printed circuit boards and electronic devices. In addition, a carbon-loaded polymer was considered as a representative lossy composite material capable of attenuating electromagnetic fields primarily through absorption mechanisms, accompanied by partial reflection effects. The selected materials represent three fundamentally different electromagnetic behaviors, namely conductive, dielectric, and lossy shielding mechanisms, enabling a comprehensive assessment of their influence on the electromagnetic performance of the mobile phone antenna.

The electromagnetic properties of the investigated materials are summarized in **Table 2**. Relative permittivity, relative permeability, and electrical conductivity were selected as the key parameters governing the interaction between the shielding structure and the electromagnetic fields generated by the mobile phone antenna. These parameters determine the dominant shielding mechanism, including reflection, absorption, and transmission of electromagnetic energy through the shielding material.

A rectangular shielding plate with dimensions of 200 mm × 200 mm was positioned near the monopole antenna in order to investigate its influence on the electromagnetic behavior of the mobile phone. The dimensions of the shielding plate were kept constant throughout the analysis, while its material properties, position, distance, and orientation relative to the antenna were varied. This approach enables the independent evaluation of each parameter and its contribution to the overall shielding performance.

Table 2
Electromagnetic properties of materials.

Material	Relative permittivity ε_r	Relative permeability μ_r	Electrical conductivity σ [S/m]
Aluminium	1	1	$3.5 \cdot 10^7$
FR4	4.4	1	0.02
Carbon-loaded polymer	10	1	100

In addition to the material properties, the relative position of the shielding plate with respect to the monopole antenna was considered as an important parameter affecting the interaction between the shielding structure and the electromagnetic fields generated by the mobile phone. Three characteristic shield positions were investigated in order to evaluate the influence of partial and complete coverage of the antenna region.

As illustrated in Fig. 2, three representative shielding configurations were considered. The first configuration corresponds to the reference case without a shielding structure. In the second configuration, the shielding plate was positioned at the center of the mobile phone model. In the third configuration, the shielding plate was shifted toward the monopole antenna, resulting in approximately 50% coverage of the mobile phone region. These configurations were selected to investigate the influence of the shielding plate location and the degree of antenna coverage on the near-field distribution and the radiation characteristics of the mobile phone antenna.

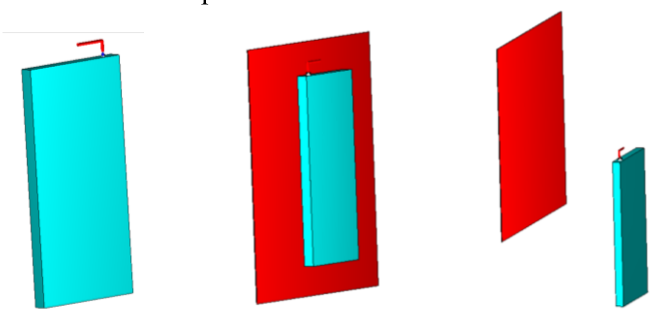

(a) (b) (c)

Fig. 2 – *Investigated shielding positions relative to the mobile phone antenna:* (a) *unshielded configuration,* (b) *centrally positioned shielding plate, and* (c) *shielding plate providing approximately* 50% *coverage of the antenna region.*

The separation distance between the shielding plate and the mobile phone antenna was also included in the parametric analysis. Three representative distances, namely 1 cm, 5 cm and 10 cm, were considered in order to investigate the influence of shield proximity on the electromagnetic behavior of the mobile phone antenna. The selected distances represent practical configurations ranging from very close proximity to moderate separation between the shielding structure and the mobile phone antenna.

Besides the shielding material, position, and separation distance, the relative orientation between the mobile phone and the shielding plate was also included in the parametric analysis. Three representative orientations were considered in order to investigate different spatial arrangements between the antenna and the shielding structure. The analyzed configurations correspond to parallel, rear-facing orientation, and orthogonal (90°) orientations, as shown in Fig. 3. These arrangements were selected to provide a comprehensive assessment of the interaction between the shielding structure and the mobile phone antenna under different geometric conditions.

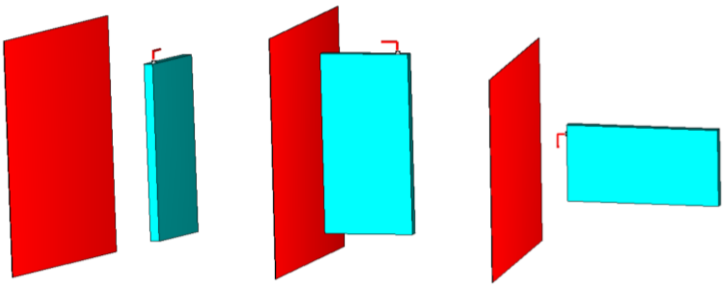

(a) (b) (c)

Fig. 3 – *Investigated mobile phone orientations relative to the shielding plate:* (a) *parallel orientation,* (b) *rear-facing orientation, and* (c) *perpendicular* (90°) *orientation.*

For each investigated configuration, both the near-field behavior and the radiation characteristics of the mobile phone antenna were evaluated. The influence of the shielding structures was assessed through the analysis of the electric field distribution, reflection coefficient S_{11}, antenna gain, and radiation patterns. These parameters provide insight into both the near-field electromagnetic behavior and the radiation characteristics of the mobile phone antenna. The adopted simulation procedure enables a comprehensive evaluation of the interaction between the shielding structures and the mobile phone antenna operating at frequencies of 1800 MHz, 2600 MHz, and 3500 MHz.

3 Results and Discussion

3.1 Near-field analysis

The electric field distribution was analyzed in order to investigate the influence of the shielding structures on the near-field behavior of the mobile phone antenna. The obtained field distributions provide insight into the spatial variation of the electromagnetic field and enable a qualitative assessment of the shielding performance. The analysis was performed using the WIPL-D electromagnetic simulation software [9], considering different shielding materials, shield positions, separation distances, and device orientations.

The results shown in Fig. 4 correspond to a parallel phone orientation, a centrally positioned shielding plate, and a shield-to-antenna distance of 10 cm. The maximum electric field value for the unshielded configuration is 5.38 V/m. The introduction of aluminum and carbon-loaded polymer shielding plates significantly reduces the maximum electric field to 2.05 V/m and 1.72 V/m, respectively, corresponding to reductions of approximately 62% and 68% compared to the unshielded case. In contrast, the FR4 shielding plate produces a maximum electric field value of 5.51 V/m, which is slightly higher than that obtained without shielding. This result indicates that the dielectric FR4 structure primarily redistributes the electromagnetic field rather than attenuating it. Consequently, the conductive shielding materials, namely aluminum and carbon-loaded polymer, provide substantially better suppression of the near-field electric field than FR4. Among the investigated materials, the carbon-loaded polymer generally exhibited a favorable compromise between shielding effectiveness and antenna performance, particularly at higher operating frequencies.

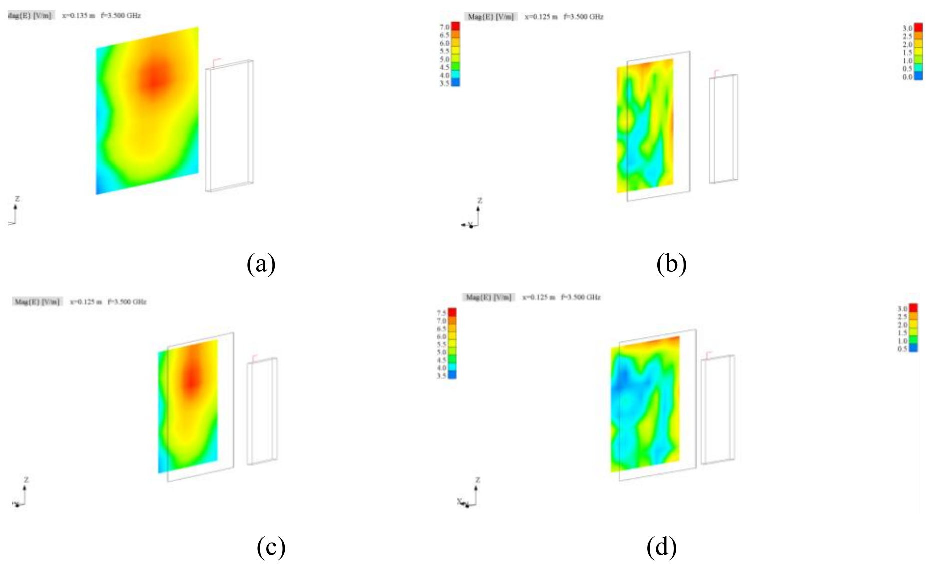

Fig. 4 – *Electric near-field distribution at* 3500 MHz *for a centrally positioned shielding plate located* 10 cm *from the mobile phone antenna in the parallel orientation:* (a) *no shielding structure,* (b) *aluminum shield,* (c) *FR4 shield, and* (d) *carbon-loaded polymer shield.*

3.2 Influence of Shield Position

In addition to the material properties and separation distance, the position of the shielding plate relative to the mobile phone antenna was also investigated. Three representative configurations were considered, namely the reference configuration without a shielding structure, a centrally positioned shielding plate, and a configuration in which the shielding plate provided approximately 50% coverage of the antenna region. The objective of this analysis was to examine how the relative location of the shielding structure affects the near-field characteristics and radiation performance of the mobile phone antenna operating at the investigated frequency bands.

Fig. 5 presents the near-field electric field distribution at 3500 MHz for three representative shielding configurations: (a) an unshielded mobile phone, (b) a centrally positioned shielding plate, and (c) shielding plate providing approximately 50% coverage of the mobile phone region. The obtained results demonstrate that the position of the shielding structure has a pronounced influence on the near-field electromagnetic behavior.

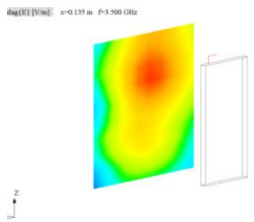

(a)

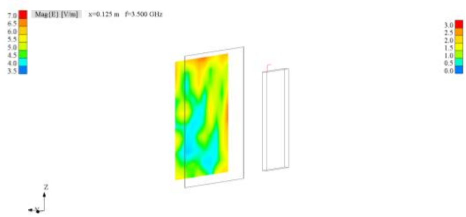

(b)

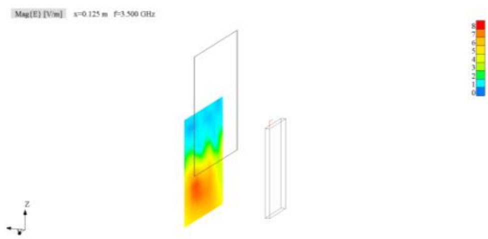

(c)

Fig. 5 – *Electric near-field distribution at* 3500 MHz *for different shielding positions using an aluminum shielding plate located* 10 cm *from the antenna in the parallel orientation:* (a) *no shield,* (b) *centrally positioned shield, and* (c) *approximately* 50% *coverage of the antenna region.*

The unshielded configuration exhibits a maximum electric field value of 4.8 V/m. When the shielding plate is positioned centrally with respect to the mobile phone antenna, the maximum electric field is significantly reduced to 0.7 V/m, indicating highly effective suppression of the near-field radiation.

In contrast, the configuration providing approximately 50% coverage results in an increased maximum electric field value of 6.1 V/m. This behavior suggests that partial coverage may lead to field concentration and redistribution effects, producing localized field enhancement rather than attenuation. Consequently, the results indicate that the effectiveness of the shielding structure is strongly dependent on its position. Among the investigated configurations, the centrally positioned shielding plate provides the most effective reduction of the near-field electric field, whereas partial coverage of the mobile phone region proves considerably less effective. The increase in the maximum electric field observed for the 50% coverage configuration can be explained by field redistribution and local field enhancement caused by the partial shielding structure. In this case, the shielding plate does not act only as an attenuating element, but also modifies the electromagnetic coupling and produces constructive interference in certain regions of the near field. As a result, localized field enhancement may occur, leading to a higher maximum electric field compared to the unshielded configuration.

3.3 Scattering parameter S_{11} analysis

The reflection coefficient S_{11} was analyzed in order to evaluate the influence of the frequency on the impedance matching characteristics of the mobile phone antenna. Variations in S_{11} provide information regarding changes in the resonant behavior and power transfer efficiency. The analysis was performed for the investigated frequencies of 1800 MHz, 2600 MHz, and 3500 MHz.

The obtained S_{11} characteristics, Fig. 6, indicate that the mobile phone antenna exhibits satisfactory impedance matching at all investigated frequencies. However, a comparison of the results reveals that the antenna achieves improved matching performance at higher operating frequencies. The minimum reflection coefficient decreases from -11.4 dB at 1800 MHz to -15.2 dB at 2600 MHz and-15.9 dB at 3500 MHz, indicating a reduction in reflected power and more efficient power transfer to the radiating element, as shown in Fig. 6. Consequently, the antenna demonstrates the best impedance matching performance in the 3500 MHz band, confirming its suitability for operation in contemporary 5G communication systems.

The influence of mobile phone orientation on the near-field electric-field distribution was investigated at 3500 MHz using an aluminum shielding plate positioned 10 cm from the antenna. Fig. 7 presents the electric-field distributions obtained for the three investigated orientations, namely parallel, rear-facing, and perpendicular (90°). The results demonstrate that the relative orientation between the mobile phone and the shielding plate has a pronounced influence on the near-field electromagnetic behavior. Significant variations in both the magnitude and spatial distribution of the electric field can be observed among the investigated configurations. The perpendicular orientation produces the strongest perturbation of the field distribution, resulting in a highly non-uniform field pattern with localized field maxima and minima. In contrast, the parallel and rear-facing configurations exhibit smoother field distributions and lower field concentrations in the vicinity of the shielding structure. These results indicate that the geometric arrangement between the mobile phone antenna and the shielding plate represents an important factor governing the near-field characteristics. Consequently, the relative orientation between the mobile phone and the shielding structure should be considered during the design and optimization of shielding solutions for mobile communication devices.

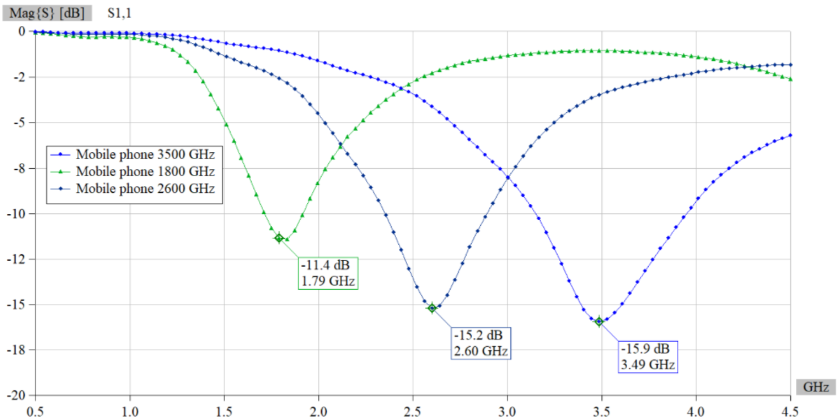

Fig. 6 – *Reflection coefficient S_{11} of the mobile phone antenna at* 1800 MHz, 2600 MHz, *and* 3500 MHz *without a shielding structure.*

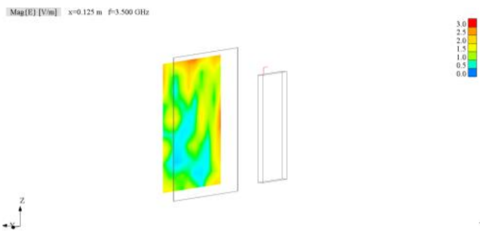

(a)

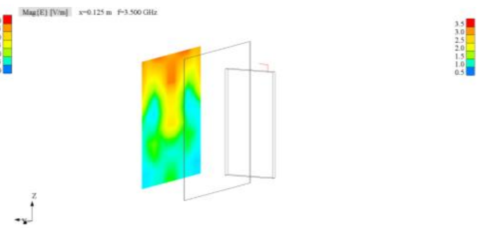

(b)

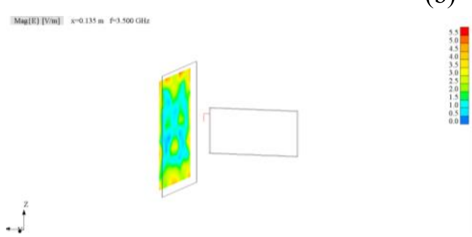

(c)

Fig. 7 – *Electric near-field distribution at* 3500 MHz *for different mobile phone orientations relative to the centrally positioned aluminum shielding plate located* 10 cm *from the antenna:* (a) *parallel orientation,* (b) *rear-facing orientation, and* (c) *perpendicular* (90°) *orientation.*

3.4 Influence of shield-to-antenna distance

In addition to the shielding material, position, and orientation, the influence of the separation distance between the mobile phone antenna and the shielding structure was also investigated. Three representative distances of 1 cm, 5 cm, and 10 cm were considered in order to evaluate the effect of the shield-to-antenna spacing on the antenna characteristics. The analysis was performed through the evaluation of the near-field distribution, reflection coefficient (S_{11}), antenna gain, and radiation patterns.

Near-field electric field distribution at 3500 MHz for different separation distances between the mobile phone antenna and the shielding plate is obtained. The maximum electric field value obtained for the unshielded configuration is 5.38 V/m. When the shielding plate is introduced, a substantial reduction of the near-field electric field is observed. For separation distances of 1 cm, 5 cm, and 10 cm, the maximum electric field values are reduced to 1.49 V/m, 1.77 V/m, and 2.19 V/m, respectively. These results clearly demonstrate that the effectiveness of the shielding structure strongly depends on its proximity to the antenna. The shortest separation distance of 1 cm provides the most effective suppression of the near-field electric field, corresponding to a reduction of approximately 72% compared to the unshielded case. As the distance between the antenna and the shielding plate increases, the shielding effect gradually decreases, leading to higher electric field levels. Therefore, the shield-to-antenna distance represents an important design parameter in the optimization of shielding structures for mobile communication devices.

The antenna gain at 3500 MHz is observed for different separation distances between the mobile phone antenna and the aluminum shielding plate. The unshielded configuration exhibits a maximum gain of 4.7 dBi. When the shielding plate is introduced, a significant reduction in antenna gain is observed as the shield approaches the antenna. For separation distances of 10 cm, 5 cm, and 1 cm, the gain decreases to 0.7 dBi, –2.0 dBi, and –4.6 dBi, respectively. These results indicate that the shielding structure strongly affects the radiation performance of the antenna. The negative gain values obtained for the 5 cm and 1 cm configurations do not imply that the antenna ceases to radiate; rather, they indicate that the radiated power in the considered direction becomes lower than that of an ideal isotropic radiator. Consequently, although a shorter shield-to-antenna distance provides more effective reduction of the near-field electric field, it also causes a substantial degradation of the antenna radiation characteristics. Therefore, the separation distance represents a critical design parameter that must be carefully optimized in order to achieve a balance between electromagnetic shielding effectiveness and antenna performance.

The results presented in **Table 3** correspond to a centrally positioned shielding plate located 1 cm from the mobile phone antenna in the parallel orientation. The electromagnetic properties of the shielding material significantly influence both the near-field and radiation characteristics of the antenna. For all investigated frequencies, the conductive aluminum and the lossy carbon-loaded polymer provide a substantial reduction of the maximum electric field compared to the unshielded configuration. The most pronounced field suppression is observed at 1800 MHz, where the maximum electric field is reduced from 6.94 V/m to 0.9 V/m and 1.3 V/m for aluminum and carbon-loaded polymer, respectively. Similar trends can be observed at 2600 MHz and 3500 MHz.

However, the reduction of the near-field electric field is accompanied by a noticeable degradation of the antenna radiation characteristics. Both aluminum and carbon-loaded polymer significantly reduce the antenna gain, indicating a strong interaction between the shielding structure and the radiating element. In contrast, the FR4 shielding plate produces only minor changes in the maximum electric field, reflection coefficient, and antenna gain, suggesting that its influence is primarily associated with field redistribution rather than effective attenuation.

Table 3

Influence of shielding material on the electromagnetic characteristics of the mobile phone antenna at 1800 MHz, 2600 MHz, *and* 3500 MHz *for a centrally positioned shielding plate located* 1 cm *from the antenna in the parallel orientation.*

Frequency [MHz]	Configuration	Material	E_{max} (V/m)	S_{11}(dB)	Gain (dBi)
1800	No shield	/	6.94	-11.4	3.1
1800	Central	Al	0.9	-10.2	-6.6
1800	Central	FR4	6.1	-11.4	2.9
1800	Central	Carbon	1.3	-30.7	-7.4
2600	No shield	/	4.82	-15.2	3.7
2600	Central	Al	2.41	-13.1	-4.5
2600	Central	FR4	5.05	-15.3	3.8
2600	Central	Carbon	1.19	-14.5	-6.4
3500	No shield	/	5.38	-15.9	4.7
3500	Central	Al	1.78	-12	-4.6
3500	Central	FR4	4.97	-16.1	4.9
3500	Central	Carbon	1.87	-16.2	2.3

Among the investigated materials, aluminum and carbon-loaded polymer provide the strongest reduction of the maximum electric field, while FR4 preserves the antenna characteristics most effectively. The carbon-loaded polymer represents an intermediate solution, offering considerable field suppression while maintaining more favorable radiation characteristics at higher frequencies. These results indicate that the selection of the shielding material involves a trade-off between near-field electric field reduction and preservation of antenna performance.

The results presented in **Table 4** demonstrate that the separation distance between the shielding plate and the mobile phone antenna has a pronounced influence on both the near-field and radiation characteristics. For all investigated frequencies, the smallest separation distance of 1 cm provides the lowest maximum electric field values, indicating the highest shielding effectiveness. However, this improvement in near-field suppression is accompanied by a significant degradation of antenna performance. As the shielding plate approaches the antenna, the antenna gain decreases considerably and the impedance matching becomes less favorable, as indicated by the higher S_{11} values. Conversely, increasing the shield-to-antenna distance leads to improved gain and better impedance matching, but also results in higher electric field levels. These results clearly reveal a trade-off between electromagnetic field reduction and antenna performance. Therefore, the shield-to-antenna distance represents a critical design parameter that must be carefully optimized in order to achieve an appropriate balance between shielding effectiveness and acceptable antenna characteristics.

Table 4

Influence of shield-to-antenna distance on the electromagnetic characteristics of the mobile phone antenna using a centrally positioned aluminum shielding plate in the parallel orientation.

Frequency [MHz]	Distance (cm)	E_{max} (V/m)	S_{11}(dB)	Gain (dBi)
1800	1	0.9	-10.2	-6.6
1800	5	9.3	-12.7	1.3
1800	10	10.9	-14.5	2.1
2600	1	2.41	-13.1	-4.5
2600	5	5.92	-15.5	2.3
2600	10	6.4	-16	3.3
3500	1	1.49	-12	-4.6
3500	5	1.77	-14.9	-2
3500	10	2.19	-16.2	0.7

The results presented in **Table 4** correspond to a centrally positioned aluminum shielding plate in the parallel orientation.

The selected results, shown in **Table 5**, illustrate the combined influence of shielding material, shield position, and mobile phone orientation on the near-field electric field, impedance matching, and antenna gain at 3500 MHz for a fixed shield-to-antenna distance of 1 cm.

Table 5

Combined influence of shielding material, shield position, and mobile phone orientation on the electromagnetic characteristics of the mobile phone antenna at 3500 MHz *for a shield-to-antenna distance of* 1 cm.

Shielding material	Shield position	*Mobile phone orientation*	E_{max} (V/m)	S_{11}(dB)	Gain (dBi)
Al	Central	Parallel	1.78	–12	–4.6
Al	Central	Rear-facing	3	–17.9	–1.4
Al	Central	Perpendicular (90°)	4.08	–17.9	–1.6
Al	50% coverage	Parallel	4.34	–16.7	2.8
Al	50% coverage	Rear-facing	2.64	–16.9	0.7
Al	50% coverage	Perpendicular (90°)	1.98	–16.9	0.7
FR4	Central	Parallel	4.97	–16.1	4.9
FR4	Central	Rear-facing	4.84	–16.1	1.8
FR4	Central	Perpendicular (90°)	5.69	–16	0.7
FR4	50% coverage	Parallel	5.8	–16	4.8
FR4	50% coverage	Rear-facing	4.51	–16.2	1.8
FR4	50% coverage	Perpendicular (90°)	5.63	–15.9	0.9
Carbon	Central	Parallel	1.24	–12.8	–5
Carbon	Central	Rear-facing	2.48	–17.3	–0.8
Carbon	Central	Perpendicular (90°)	2.61	–17.5	–1
Carbon	50% coverage	Parallel	2.99	–16.5	1.9
Carbon	50% coverage	Rear-facing	1.75	–16.3	–2.7
Carbon	50% coverage	Perpendicular (90°)	8.1	–16.8	0.5

The results presented in **Table 5** demonstrate that the electromagnetic behavior of the mobile phone antenna is strongly affected by the combined influence of shielding material, shield position, and mobile phone orientation. Among the investigated configurations, the carbon-loaded polymer with a centrally positioned shield and parallel phone orientation provides the lowest maximum electric field (1.24 V/m), followed by aluminum (1.78 V/m), whereas FR4 yields considerably higher values (4.97 V/m). However, this improvement is accompanied by a noticeable reduction in antenna gain, reaching −5.0 dBi for the carbon-loaded polymer and −4.6 dBi for aluminum, while FR4 preserves a substantially higher gain of 4.9 dBi under the same configuration. Changing the shield position and mobile phone orientation significantly modifies both the electric-field distribution and antenna characteristics. For example, the carbon-loaded polymer with 50% shield coverage and perpendicular orientation produces the highest electric-field value (8.1 V/m), indicating that certain combinations of material properties and geometric configuration may lead to localized field enhancement despite the presence of the shielding structure. These results demonstrate that an effective shielding solution cannot be selected solely on the basis of electric-field reduction, but requires simultaneous consideration of antenna matching, radiation performance, and shielding effectiveness.

4 Conclusion

This paper presented a numerical investigation of the influence of shielding structures on the near-field and radiation characteristics of a mobile phone antenna operating in representative 4G and 5G communication bands at 1800 MHz, 2600 MHz, and 3500 MHz. Electromagnetic simulations were performed using the WIPL-D software in order to evaluate the effects of shielding material, shield position, orientation, and shield-to-antenna distance.

The obtained results showed that the antenna exhibits satisfactory impedance matching at all investigated frequencies, with improved matching performance at higher frequencies. The lowest reflection coefficient was achieved at 3500 MHz, indicating the most favorable impedance matching and the most efficient power transfer to the radiating element.

The analysis demonstrated that both the electromagnetic properties of the shielding material and the geometric configuration of the shielding structure significantly influence the near-field and radiation characteristics of the mobile phone antenna. Aluminum and carbon-loaded polymer shielding structures provided a substantial reduction of the maximum electric field, whereas the FR4 shielding plate mainly caused field redistribution and produced only limited attenuation of the near-field intensity. Furthermore, the results revealed that the position of the shielding structure plays a critical role in determining its effectiveness. While a centrally positioned shielding plate significantly reduced the electric field, partial coverage of the antenna region may lead to field redistribution and localized field enhancement.

The shield-to-antenna distance was identified as one of the most important design parameters. Reducing the separation distance resulted in a significant decrease of the maximum electric field, indicating improved shielding effectiveness. However, this improvement was accompanied by a noticeable degradation of antenna gain and impedance matching. Consequently, the results clearly demonstrate the existence of a trade-off between electromagnetic field suppression and preservation of antenna performance.

Overall, the presented study confirms that the effectiveness of shielding structures cannot be assessed solely through electric field reduction. Effective shielding design for mobile communication devices requires simultaneous optimization of material properties and geometric configuration in order to achieve substantial near-field field suppression while maintaining acceptable antenna characteristics. Considering both the near-field suppression and antenna characteristics, the carbon-loaded polymer exhibited the most balanced compromise between shielding effectiveness and antenna performance, particularly at higher operating frequencies.

Future work will include SAR analysis and the incorporation of realistic human head and hand models in order to evaluate the interaction between shielding structures and human exposure under practical operating conditions.

5 Acknowledgments

This study was supported by the Ministry of Science, Technological Development and Innovation of the Republic of Serbia and these results are parts of the Grant No. 451-03-136/2025-03/200132 with University of Kragujevac – Faculty of Technical Sciences Čacak.

6 References

[1] J. G. Andrews, S. Buzzi, W. Choi, S. V. Hanly, A. Lozano, A. C. K. Soong, J. C. Zhang: What Will 5G Be?, IEEE Journal on Selected Areas in Communications, Vol. 32, No. 6, June 2014, pp. 1065 – 1082.

[2] A. Osseiran, F. Boccardi, V. Braun, K. Kusume, P. Marsch, M. Maternia, O. Queseth, M. Schellmann, H. Schotten, H. Taoka, H. Tullberg, M. A. Uusitalo, B. Timus, M. Fallgren: Scenarios for 5G Mobile and Wireless Communications: The Vision of the METIS Project, IEEE Communications Magazine, Vol. 52, No. 5, May 2014, pp. 26 – 35.

[3] Base Station (BS) Radio Transmission and Reception, 3GPP TS 38.104, NR, Release 18, v18.10.0, 3rd Generation Partnership Project, 2025.

[4] T. S. Rappaport: Wireless Communications: Principles and Practice, 2nd Edition, Prentice Hall, Upper Saddle River, 2002.

[5] K. Karipidis, R. Mate, D. Urban, R. Tinker, A. Wood: 5G Mobile Networks and Health – A State-of-the-Science Review of the Research into Low-Level RF Fields Above 6 GHz, Journal of Exposure Science & Environmental Epidemiology, Vol. 31, No. 4, July 2021, pp. 585 – 605.

[6] D. B. Deaconescu, A. M. Buda, D. Vatamanu, S. Miclaus: The Dynamics of the Radiated Field Near a Mobile Phone Connected to a 4G or 5G Network, Engineering, Technology and Applied Science Research, Vol. 12, No. 1, February 2022, pp. 8101 – 8106.

[7] A. Hirata, S. Kodera, K. Sasaki, J. Gomez-Tames, I. Laakso, A. Wood, S. Watanabe, K. R. Foster: Human Exposure to Radiofrequency Energy Above 6 GHz: Review of Computational Dosimetry Studies, Physics in Medicine & Biology, Vol. 66, No. 8, 2021, p. 08TR01.

[8] C. R. Paul: Introduction to Electromagnetic Compatibility, 2nd Edition, John Wiley & Sons, Inc., Hoboken, 2006.

[9] WIPL-D, Belgrade, Serbia: WIPL-D Pro 21.0, 3D Electromagnetic Solver, 2025, Available at: http://wipl-d.com.

[10] S. S. Pudipeddi, P. V. Y. Jayasree, S. G. Chintala: Polarization Effect Assessment of Sub-6 GHz Frequencies on Adult and Child Four-Layered Head Models, Engineering, Technology & Applied Science Research, Vol. 12, No. 4, August 2022, pp. 8954 – 8959.

[11] U. Jovanović, D. Zigar, J. Malenović-Nikolić, D. Krstić: Assessing SAR1g Distribution in the Human Head During Hands-Free Mobile Phone Usage, Serbian Journal of Electrical Engineering, Vol. 21, No. 1, February 2024, pp. 135 – 147.

[12] A. K. Penta, C. R. Phani Kumar: A Novel PIFA Design for SAR Reduction in 5G Networks to Analyze the RF Shield Impact, Engineering, Technology & Applied Science Research, Vol. 14, No. 3, June 2024, pp. 14102 – 14108.

[13] J. Acharjee, J. Ali, M. Uzair, T. Phakaew, P. Akkaraekthalin, Y. Maiket, R. Yeetsorn, S. Chalermwisutkul: Metasurface-Loaded Biodegradable Mobile Phone Back Cover for Enhanced Radiation Performance, Materials, Vol. 18, No. 4, February 2025, p. 730.

[14] N. H. Jemaludin, A. J. A. Al-Gburi, R. H. Elabd, T. Saeidi, M. F. Akbar, I. M. Ibrahim, Z. Zakaria: A Comprehensive Review on MIMO Antennas for 5G Smartphones: Mutual Coupling Techniques, Comparative Studies, SAR Analysis, and Future Directions, Results in Engineering, Vol. 23, September 2024, p. 102712.

[15] B. Park, S. Hwang, H. Lee, Y. Jung, T. Kim, S. J. Kwon, D. Jung, S.- B. Lee: Absorption-Dominant Electromagnetic Interference (EMI) Shielding across Multiple mmWave Bands Using Conductive Patterned Magnetic Composite and Double-Walled Carbon Nanotube Film, Advanced Functional Materials, Vol. 34, No. 40, October 2024, p. 2406197.

[16] Y. Wang, L. Sun, Z. Du, Z. Zhang: Antenna Design for Modern Mobile Phones: A Review, Electromagnetic Science, Vol. 2, No. 2, June 2024, p. 0060521.